Quasi-Elastic Lepton Nucleus Scattering and the Correlated Fermi Gas Model (arXiv: 2405.05342)

Bhubanjyoti Bhattacharya[1,2] Sam Carey[2] Erez O. Cohen[3] Gil Paz[2]

Lawrence Technological University (Michigan, USA)[1],
Wayne State University (Michigan, USA)[2],
Nuclear Research Center - Negev (Beer-Sheva, Israel)[3]

September 16, 2024

Motivation

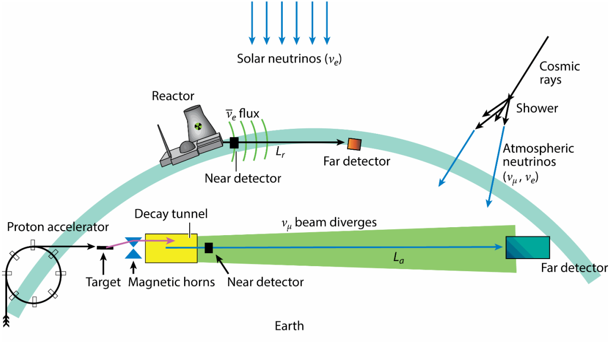

Figure: Neutrino sources (M.V. Diwan, *et al.*, Ann. Rev. Nucl. Part. Sci. **66**, 47 (2016))

- Current and future neutrino experiments (e.g. MicroBooNE, Minerva, T2K, DUNE) aim to:
  - Precisely measure Standard Model parameters
  - Address questions: mass hierarchy, nature of ν, δ_{CP}
  - Uncover non-standard neutrino interactions (NSI)

Motivation

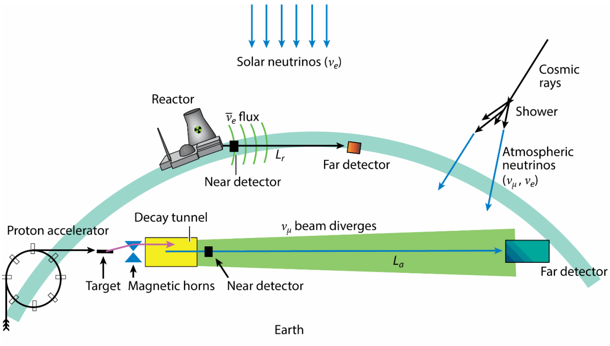

Figure: Neutrino sources (M.V. Diwan, *et al.*, Ann. Rev. Nucl. Part. Sci. **66**, 47 (2016))

- Current and future neutrino experiments (e.g. MicroBooNE, Minerva, T2K, DUNE) aim to:
  - Precisely measure Standard Model parameters
  - Address questions: mass hierarchy, nature of ν, δ_{CP}
  - Uncover non-standard neutrino interactions (NSI)
- Reducing uncertainty on the lepton-nucleus interactions to meet the physics goals in the precision era.

Lepton-Nucleus QE Scattering

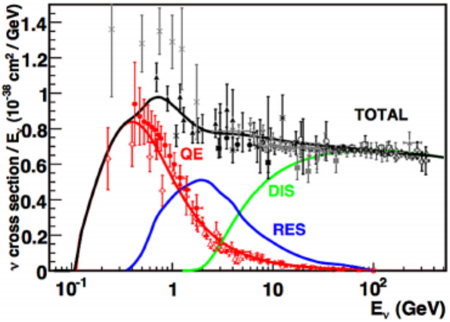

Figure: Total ν per nucleon CC cross sections
(Formaggio and Zeller, Rev. Mod. Phys. **84**, 1307 (2012))

- CCQE dominates cross-section at energies of interest for oscillation experiments.

Lepton-Nucleus QE Scattering

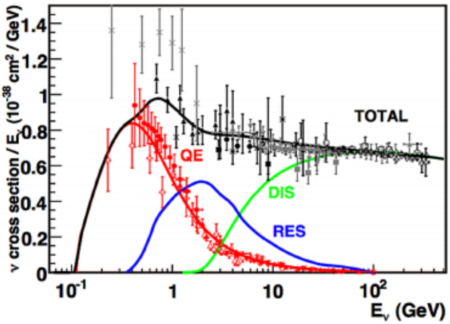

Figure: Total ν per nucleon CC cross sections
(Formaggio and Zeller, Rev. Mod. Phys. **84**, 1307 (2012))

- CCQE dominates cross-section at energies of interest for oscillation experiments.
- Cross-section for neutrino scattering off nucleus determined by folding lepton-quark interaction twice.

Lepton-Nucleus QE Scattering

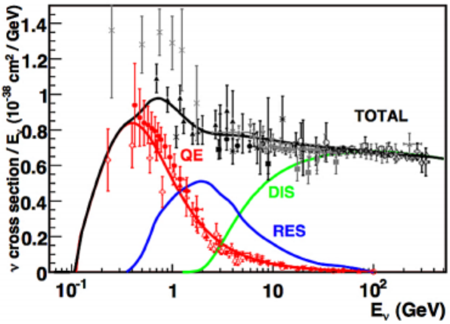

Figure: Total ν per nucleon CC cross sections
(Formaggio and Zeller, Rev. Mod. Phys. **84**, 1307 (2012))

- CCQE dominates cross-section at energies of interest for oscillation experiments.
- Cross-section for neutrino scattering off nucleus determined by folding lepton-quark interaction twice.
  1. nucleon form factors: lepton-quark interaction ⇒ lepton-nucleon interaction ($\nu_\mu\, n \to \mu^-\, p$)

Lepton-Nucleus QE Scattering

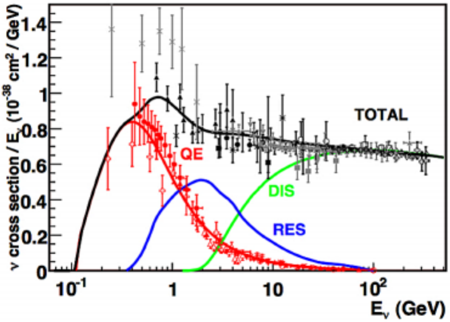

Figure: Total ν per nucleon CC cross sections
(Formaggio and Zeller, Rev. Mod. Phys. **84**, 1307 (2012))

- CCQE dominates cross-section at energies of interest for oscillation experiments.
- Cross-section for neutrino scattering off nucleus determined by folding lepton-quark interaction twice.
  1. nucleon form factors: lepton-quark interaction $\Rightarrow$ lepton-nucleon interaction ($\nu_\mu\, n \to \mu^-\, p$)
  2. nuclear model: nucleon $\Rightarrow$ nuclear level ($\nu_\mu\, X_Z^A \to \mu^-\, p\, X_Z^{A-1}$)

Lepton-nucleon scattering process

Cross-section of Lepton-nucleon scattering

Bhattacharya, Hill and Paz, Phys. Rev. D, **84**, 073006 (2011)

For the process:

$$l(k) + N(p) \to l'(k') + N'(p')$$

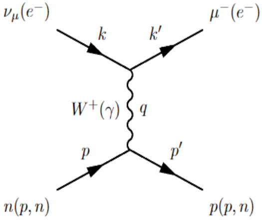

- For the Weak/Electromagnetic interaction, the Lagrangian is:

$$\mathscr{L} \quad = \quad \mathcal{C}_{Weak,EM} \bar{l}' \gamma^{\mu}(1-\gamma_5) l \bar{q}_i \gamma_{\mu}(1-\gamma_5) q_j, \ \left\{ \mathcal{C}_{Weak,EM} = \frac{G_F}{\sqrt{2}} V_{ij}, \ \frac{e^2}{q^2} \right\}$$

Cross-section of Lepton-nucleon scattering

Bhattacharya, Hill and Paz, Phys. Rev. D, **84**, 073006 (2011)

For the process:

$$l(k) + N(p) \to l'(k') + N'(p')$$

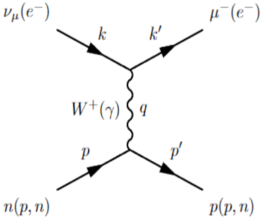

- For the Weak/Electromagnetic interaction, the Lagrangian is:

$$\mathscr{L} \quad = \quad \mathcal{C}_{Weak,EM}\bar{l}'\gamma^{\mu}(1-\gamma_5)l\bar{q}_i\gamma_{\mu}(1-\gamma_5)q_j, \ \left\{\mathcal{C}_{Weak,EM} = \frac{G_F}{\sqrt{2}}V_{ij}, \ \frac{e^2}{q^2}\right\}$$

- The cross-section for the lepton-nucleon scattering:

$$\sigma_{nucleon} = \frac{\bar{\mathcal{C}}^2_{EM,Weak}}{4|k.p|}\int \frac{d^3k'}{(2\pi)^3 2E_{k'}} L^{\mu\nu}\int \frac{d^3p'}{(2\pi)^3 2E_{p'}}(2\pi)^4\delta^4(p-p'+q)H_{\mu\nu}$$

Free nucleon cross-section

- nucleon tensor

$$H_{\mu\nu} = Tr[(\not{p}' + m_N)\Gamma_\mu(q)(\not{p} + m_N)\bar{\Gamma}_\nu(q)]$$

with the following decomposition:

$$H_{\mu\nu} = -g_{\mu\nu}H_1 + \frac{p_\mu p_\nu}{m_N^2}H_2 - i\frac{\epsilon_{\mu\nu\rho\sigma}}{2m_N^2}p^\rho q^\sigma H_3 + \frac{q_\mu q_\nu}{m_N^2}H_4 + \frac{(p_\mu q_\nu + q_\mu p_\nu)}{2m_N^2}H_5\,.$$

Free nucleon cross-section

- nucleon tensor

$$H_{\mu\nu} = Tr[(\not{p}' + m_N)\Gamma_\mu(q)(\not{p} + m_N)\bar{\Gamma}_\nu(q)]$$

with the following decomposition:

$$H_{\mu\nu} = -g_{\mu\nu} H_1 + \frac{p_\mu p_\nu}{m_N^2} H_2 - i\frac{\epsilon_{\mu\nu\rho\sigma}}{2m_N^2} p^\rho q^\sigma H_3 + \frac{q_\mu q_\nu}{m_N^2} H_4 + \frac{(p_\mu q_\nu + q_\mu p_\nu)}{2m_N^2} H_5 \,.$$

- $\Gamma_\mu(q)$ defined via the matrix element of the EM or weak current as:

$$\left\langle N(p') \right| \bar{q}_i \gamma_\mu (1 - \gamma_5) q_j \left| N(p) \right\rangle = \bar{u}(p')\Gamma_\mu(q) u(p)$$

where $q = k - k' = p' - p$

Free nucleon cross-section

- nucleon tensor

$$H_{\mu\nu} = Tr[(\not{p}' + m_N)\Gamma_\mu(q)(\not{p} + m_N)\bar{\Gamma}_\nu(q)]$$

  with the following decomposition:

$$H_{\mu\nu} = -g_{\mu\nu} H_1 + \frac{p_\mu p_\nu}{m_N^2} H_2 - i\frac{\epsilon_{\mu\nu\rho\sigma}}{2m_N^2} p^\rho q^\sigma H_3 + \frac{q_\mu q_\nu}{m_N^2} H_4 + \frac{(p_\mu q_\nu + q_\mu p_\nu)}{2m_N^2} H_5 \, .$$

- $\Gamma_\mu(q)$ defined via the matrix element of the EM or weak current as:

$$\left\langle N(p')\right| \bar{q}_i \gamma_\mu (1-\gamma_5) q_j \left|N(p)\right\rangle = \bar{u}(p')\Gamma_\mu(q) u(p)$$

  where $q = k - k' = p' - p$

- The vertex function can be expressed in terms of the form factors as:

$$\Gamma_\mu(q) = \gamma_\mu F_1(q^2) + \frac{i}{2m_N}\sigma_{\mu\nu} q^\nu F_2(q^2) + \gamma_\mu\gamma_5 F_A(q^2) + \frac{q_\mu}{m_N}\gamma_5 F_P(q^2) \, ,$$

Vector form factor (F_1, F_2)

1. BBBA: The functional form for this parameterization is given by (Bradford, Bodek, Budd and Arrington, Nucl. Phys. B Proc. Suppl., **159**:127–132 (2006))

$$G^{p,n}_{E/M} = \frac{\sum_{k=0}^{2} a_k \tau^k}{1 + \sum_{k=1}^{4} b_k \tau^k} \quad (\text{where } \tau = \frac{-q^2}{4m_N^2})$$

2. BHLT: Determined from a global fit to electron scattering data. Expressed as convergent expansion variable $z(q^2)$
(Borah, Hill, Lee and Tomalak, Phys. Rev. D, **102**(7):074012, (2020))

$$G^{p,n}_{E} = \sum_{k=0}^{k_{max}} a_k z(q^2)^k,$$

$$G^{p,n}_{M} = G^{p,n}_{M}(0) \sum_{k=0}^{k_{max}} b_k z(q^2)^k,$$

$$z(q^2) = \frac{\sqrt{t_{cut} - q^2} - \sqrt{t_{cut} - t_0}}{\sqrt{t_{cut} - q^2} + \sqrt{t_{cut} - t_0}}$$

where, $t_{cut} = 4m_\pi^2$ and $t_0 = -0.21\,\text{GeV}^2$.

Vector form factor (F_1, F_2)

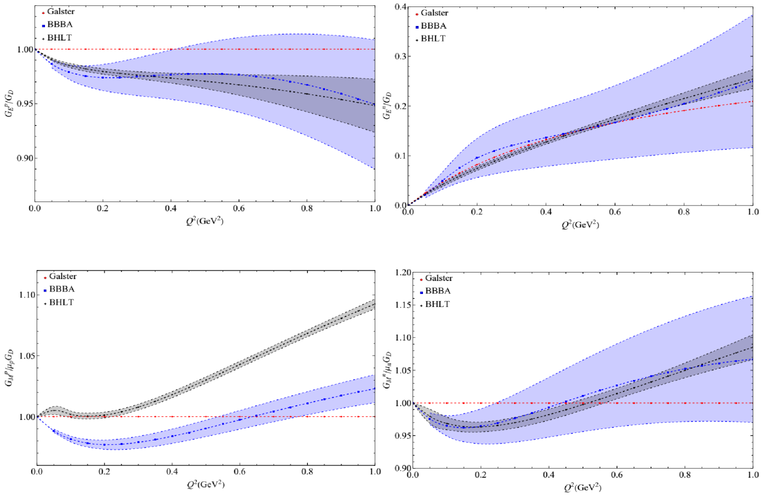

Axial-Vector form factor (F_A, F_P)

- The various axial-vector form factor models were extracted by using the z-expansion formalism. While, F_P is related to F_A by PCAC.

Scattering data:

1. MBGH: Determined from charged-current neutrino-deuterium scattering data (Meyer, Betancourt, Gran, and Hill, Phys. Rev. D, **93**(11):113015, (2016)).
2. MINERvA: Extracted from the $\bar{\nu}$-hydrogen scattering using the plastic scintillator target of MINERvA experiment (Cai, *et al.*, Nature, **614**(7946):48–53, (2023)).

Lattice QCD:

3. NME 22: (Park, *et al.*, Phys. Rev. D, **105**(5):054505, (2022))
4. Mainz 22: (Djukanovic, *et al.*, Phys. Rev. D, **106**(7):074503, (2022))
5. PNDME 23: (Jang, *et al.*, Phys. Rev. D, **109**(1):014503, (2024))
6. ETMC 23: (Alexandrou, *et al.*, Phys. Rev. D, **109**(3):034503, (2024))
7. RQCD 20: (Bali, *et al.*, JHEP, **05**:126, (2020))

Axial-Vector form factor (F_A, F_P)

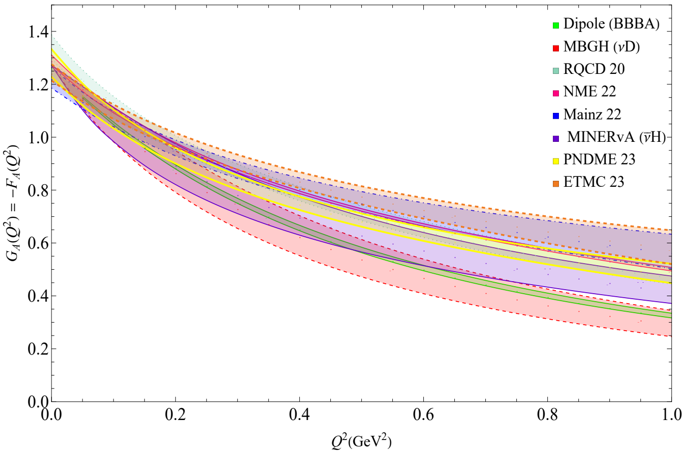

Lepton-Nuclear Scattering Process

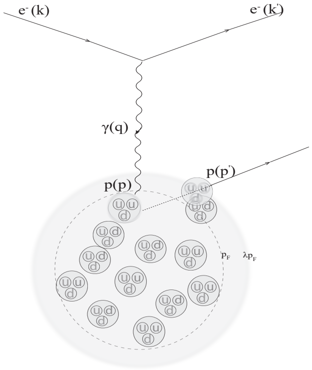

- Cross-section for lepton-nuclear scattering: convolution of free cross-section with nuclear distributions:

$$\sigma_{\text{nuclear}} = n_i(\boldsymbol{p}) \otimes \sigma_{\text{nucleon}}(\boldsymbol{p} \to \boldsymbol{p}') \otimes [1 - n_f(\boldsymbol{p}')],$$

$$d\sigma_{nuclear} = \frac{\mathcal{C}^2_{Weak,EM}}{|k \cdot p|} \frac{d^3k'}{2E_{k'}} L^{\mu\nu} W_{\mu\nu}$$

Relativistic Fermi Gas

Relativistic Fermi Gas

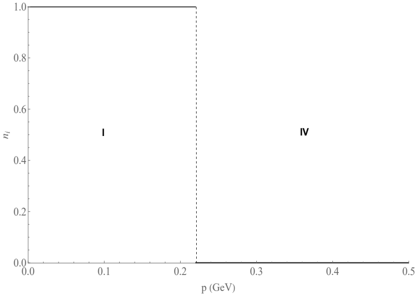

Figure: RFG momentum distribution

- Distribution of neutrons and protons in the model:
$$n^{RFG}(\boldsymbol{p}) = \theta(p_F - |\boldsymbol{p}|).$$
- Commonly used; nucleons: non-interacting Fermi gas in nucleus.

Relativistic Fermi Gas

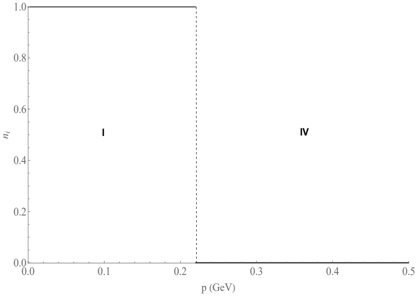

Figure: RFG momentum distribution

- Distribution of neutrons and protons in the model:
$$n^{RFG}(\boldsymbol{p}) = \theta(p_F - |\boldsymbol{p}|).$$
- Commonly used; nucleons: non-interacting Fermi gas in nucleus.
- Nucleons occupy all available energy states up to the maximum one, the Fermi energy E_F.

Correlated Fermi Gas

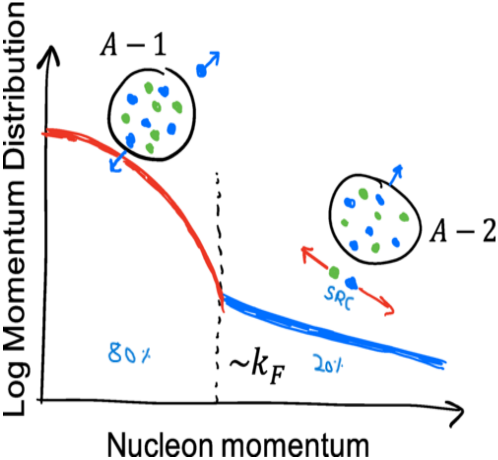

Figure: Inclusive and Exclusive electron scattering experiment observation of SRC pairs (Tropiano, Bogner and Furnstahl, Phys. Rev. C **104**, 034311 (2021))

Correlated Fermi Gas

Hen, Li, Guo, Weinstein and Piasetzky, Phys. Rev. C, **91**, 025803 (2015):

$$n^{\mathrm{CFG}}(\boldsymbol{p}) = \begin{cases} 1 - \left(1 - \frac{1}{\lambda}\right)\frac{c_0}{\pi^2} \equiv \alpha_0 & |\boldsymbol{p}| \leq p_F \\ \frac{c_0}{3\pi^2}\left(\frac{p_F}{\boldsymbol{p}}\right)^4 \equiv \frac{\alpha_1}{|\boldsymbol{p}|^4} & p_F \leq |\boldsymbol{p}| \leq \lambda p_F \\ 0 & |\boldsymbol{p}| \geq \lambda p_F. \end{cases}$$

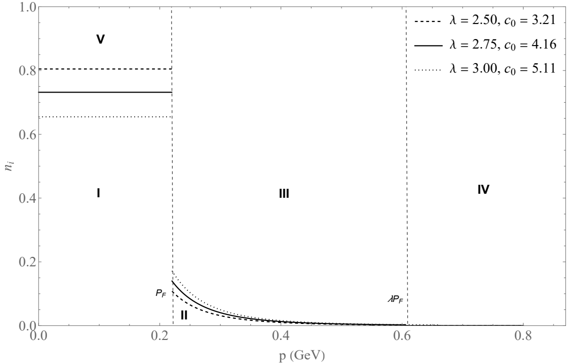

Figure: CFG momentum distributions

Phase space integrals

- The nuclear structure function:

$$W_{\mu\nu} = \int d^3p\ f(\mathbf{p}, q^0, \mathbf{q}) H_{\mu\nu}(\epsilon_p, \mathbf{p}; q^0, \mathbf{q}),$$

expanded similar to hadronic tensor,

$$W_{\mu\nu} = -g_{\mu\nu} W_1 + \frac{p_\mu^T p_\nu^T}{m_T^2} W_2 - \frac{i\epsilon_{\mu\nu\rho\sigma} p_T^\rho p_T^\sigma}{2m_T^2} W_3 + \frac{q_\mu q_\nu}{m_T^2} W_4 + \frac{p_\mu^T q_\nu + q_\mu p_\nu^T}{2m_T^2} W_5$$

Phase space integrals

- The nuclear structure function:

$$W_{\mu\nu} = \int d^3p\ f(\mathbf{p}, q^0, \mathbf{q}) H_{\mu\nu}(\epsilon_p, \mathbf{p}; q^0, \mathbf{q}),$$

expanded similar to hadronic tensor,

$$W_{\mu\nu} = -g_{\mu\nu} W_1 + \frac{p_\mu^T p_\nu^T}{m_T^2} W_2 - \frac{i\epsilon_{\mu\nu\rho\sigma} p_T^\rho p_T^\sigma}{2m_T^2} W_3 + \frac{q_\mu q_\nu}{m_T^2} W_4 + \frac{p_\mu^T q_\nu + q_\mu p_\nu^T}{2m_T^2} W_5$$

- The W_i's are written in terms of the H_i's and the phase-space integrals a_i's,

$$\begin{aligned}
W_1 &= a_1 H_1 + \frac{1}{2}(a_2 - a_3) H_2\,, \\
W_2 &= \left[a_4 + \frac{\omega^2}{|\boldsymbol{q}|^2} a_3 - 2\frac{\omega}{|\boldsymbol{q}|} a_5 + \frac{1}{2}\left(1 - \frac{\omega^2}{|\boldsymbol{q}|^2}\right)(a_2 - a_3)\right] H_2\,, \\
W_3 &= \frac{m_T}{m_N}\left(a_7 - \frac{\omega}{|\boldsymbol{q}|} a_6\right) H_3\,, \\
W_4 &= \frac{m_T^2}{m_N^2}\left[a_1 H_4 + \frac{m_N}{|\boldsymbol{q}|} a_6 H_5 + \frac{m_N^2}{2|\boldsymbol{q}|^2}(3a_3 - a_2) H_2\right]\,, \\
W_5 &= \frac{m_T}{m_N}\left(a_7 - \frac{\omega}{|\boldsymbol{q}|} a_6\right) H_5 + \frac{m_T}{|\boldsymbol{q}|}\left[2a_5 + \frac{\omega}{|\boldsymbol{q}|}(a_2 - 3a_3)\right] H_2\,,
\end{aligned} \tag{1}$$

Phase space integrals

- The a_i's are written in terms of the distribution function:

$$
\begin{aligned}
a_1 &= \int d^3\mathbf{p}\ f(\mathbf{p}, q^0, \mathbf{q})\ , \\
a_2 &= \int d^3\mathbf{p}\ f(\mathbf{p}, q^0, \mathbf{q})\ \frac{|\mathbf{p}|^2}{m_N^2}\ , \\
a_3 &= \int d^3\mathbf{p}\ f(\mathbf{p}, q^0, \mathbf{q})\ \frac{p_z^2}{m_N^2}\ , \\
a_4 &= \int d^3\mathbf{p}\ f(\mathbf{p}, q^0, \mathbf{q})\ \frac{\epsilon_{\mathbf{p}}^2}{m_N^2}\ , \\
a_5 &= \int d^3\mathbf{p}\ f(\mathbf{p}, q^0, \mathbf{q})\ \frac{\epsilon_{\mathbf{p}} p_z}{m_N^2}\ . \\
a_6 &= \int d^3\mathbf{p}\ f(\mathbf{p}, q^0, \mathbf{q})\ \frac{p^z}{m_N}\ . \\
a_7 &= \int d^3\mathbf{p}\ f(\mathbf{p}, q^0, \mathbf{q})\ \frac{\epsilon_{\mathbf{p}}}{m_N^2}\ .
\end{aligned}
$$

Limits of integration: CFG (I → III)

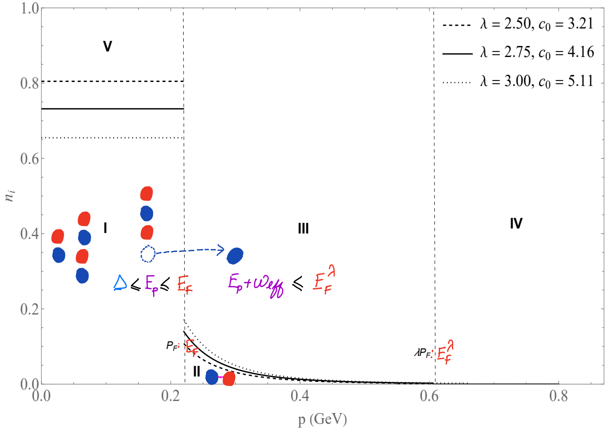

$$\text{I} \rightarrow \text{III}: \quad E_{\text{low}} = \max\left(\Delta, E_F - \omega_{eff}\right), \quad E_{\text{high}} = \min\left(E_F, E_F^{\lambda} - \omega_{eff}\right).$$

Limits of integration: CFG

- **I** $\rightarrow$ **III**:

$$E_{\text{low}} = \max\left(\Delta, E_F - \omega_{\text{eff}}\right), \quad E_{\text{high}} = \min\left(E_F, E_F^{\lambda} - \omega_{\text{eff}}\right).$$

- **I** $\rightarrow$ **IV**:

$$E_{\text{low}} = \max\left(\Delta, E_F^{\lambda} - \omega_{\text{eff}}\right), \quad E_{\text{high}} = E_F.$$

- **I** $\rightarrow$ **V**:

$$E_{\text{low}} = \max\left(\Delta, -\omega_{\text{eff}}\right), \quad E_{\text{high}} = \min\left(E_F, E_F - \omega_{\text{eff}}\right).$$

- **II** $\rightarrow$ **III**:

$$E_{\text{low}} = \max\left(\Delta, E_F, E_F - \omega_{\text{eff}}\right), \quad E_{\text{high}} = \min\left(E_F^{\lambda}, E_F^{\lambda} - \omega_{\text{eff}}\right)$$

- **II** $\rightarrow$ **IV**:

$$E_{\text{low}} = \max\left(\Delta, E_F, E_F^{\lambda} - \omega_{\text{eff}}\right), \quad E_{\text{high}} = E_F^{\lambda}.$$

- **II** $\rightarrow$ **V**:

$$E_{\text{low}} = \max\left(\Delta, E_F, -\omega_{\text{eff}}\right), \quad E_{\text{high}} = \min\left(E_F^{\lambda}, E_F - \omega_{\text{eff}}\right).$$

Differential cross-section

- In the rest frame of the nucleon, let $E_l(=|P_l|$ for $m_{e,\nu} \approx 0)$ be the energy of the outgoing charged lepton, and θ_l be the angle between incoming and outgoing lepton.

$$\frac{d\sigma^e_{nuclear}}{d\Omega_\ell dE_\ell} = \frac{\alpha^2 E_\ell^2}{4\pi Q^4 m_T}\left[2W_1(1-\cos\theta_\ell) + W_2(1+\cos\theta_\ell)\right]$$

$$\frac{d\sigma^\nu_{\mathrm{nuclear}}}{d\Omega_\ell dE_\ell} = \frac{G_F^2|\vec{P}_\ell|}{32\pi^3\, m_T}\Bigg\{2(E_\ell - |\vec{P}_\ell|\cos\theta_\ell)\, W_1 + (E_\ell + |\vec{P}_\ell|\cos\theta_\ell) W_2$$

$$\pm\frac{1}{m_T}\left[(E_\ell - |\vec{P}_\ell|\cos\theta_\ell)(E_\nu + E_\ell) - m_\ell^2\right] W_3 + \frac{m_\ell^2}{m_T^2}(E_\ell - |\vec{P}_\ell|\cos\theta_\ell) W_4 - \frac{m_\ell^2}{m_T}\, W_5\Bigg\},$$

- To calculate the cross-section we add all the possible transitions, namely,

$$d\sigma = d\sigma_{I\to III} + d\sigma_{I\to IV} + d\sigma_{I\to V} + d\sigma_{II\to III} + d\sigma_{II\to IV} + d\sigma_{II\to V}.$$

Results

Electron Scattering: 480 MeV; 60°

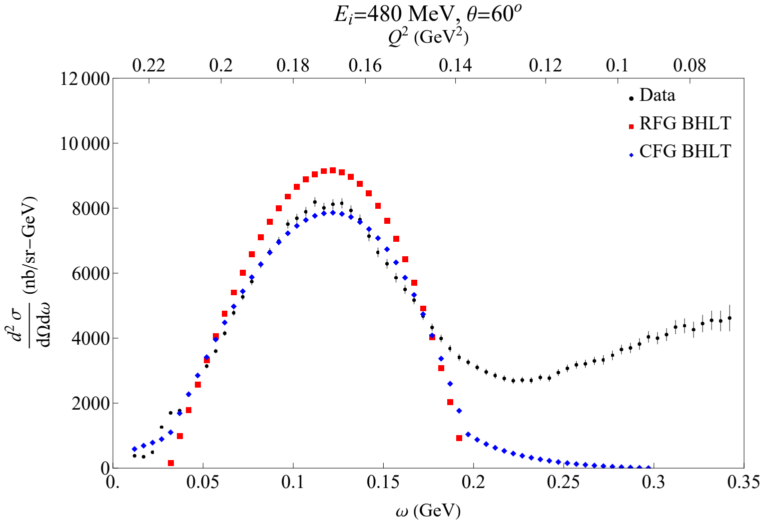

- **Fix vector form factor** and **vary nuclear models** in comparison with carbon data (http://discovery.phys.virginia.edu/research/groups/qes-archive).

Electron Scattering: 480 MeV; 60° (by transitions)

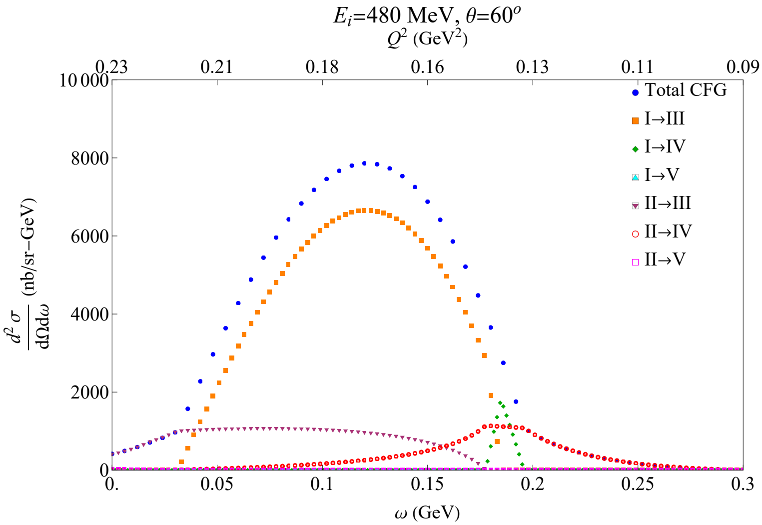

Electron Scattering: 680 MeV; 36°, 60°

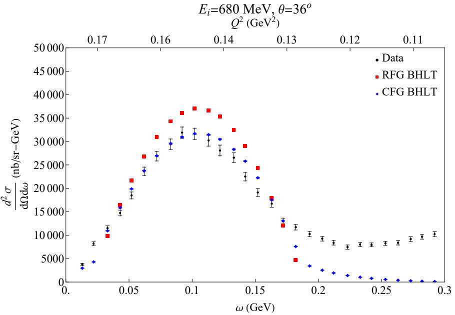

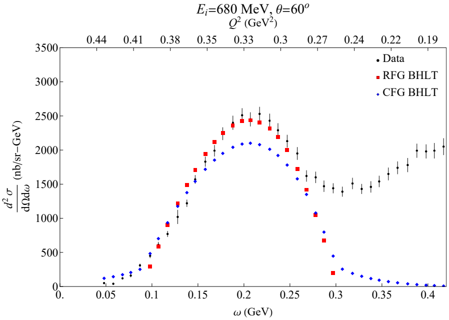

Electron Scattering: Form factor comparison

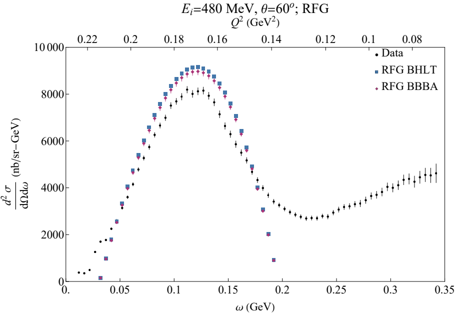

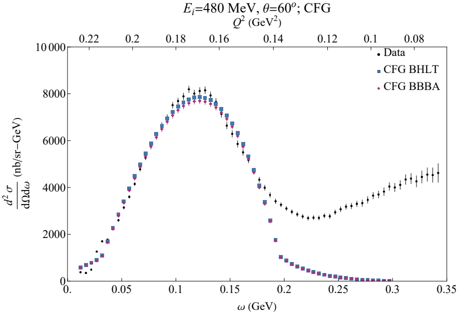

- **Fix nuclear model** and **vary form factor** models: BBBA and BHLT.
- Observe: differences from the form factors models small compared to differences between RFG and CFG.

Neutrino Scattering: Before flux averaging

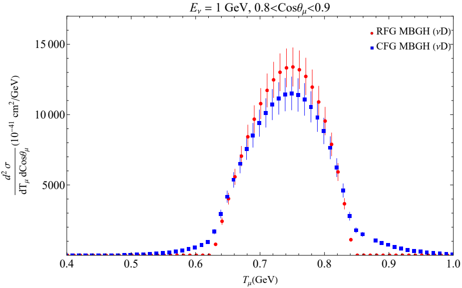

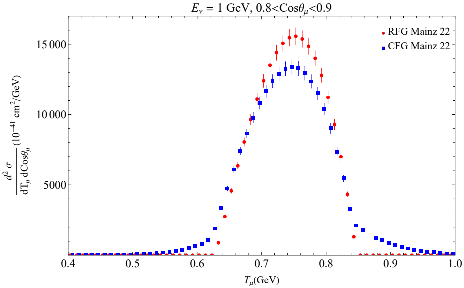

Where, $T_\mu = E_\nu - m_\mu - \omega$

- Hypothetical scenario: fixed neutrino energy.
- F_1 and F_2: BHLT parameterization, F_A: MBGH and Mainz22.

Neutrino Scattering: After flux averaging

The neutrino cross-section is convoluted with the neutrino flux distribution:

$$\frac{d\sigma_{\text{carbon,per nucleon,avg.}}}{dE_\ell d\cos\theta_\ell} = \int dE_\nu\, f(E_\nu)\, \frac{d\sigma_{\text{carbon,per nucleon}}}{dE_\ell d\cos\theta_\ell}.$$

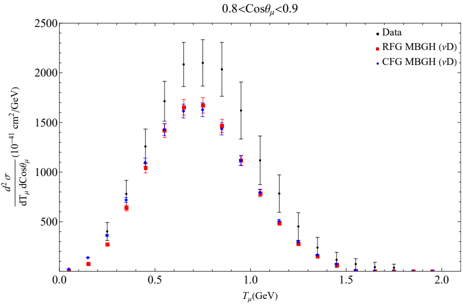

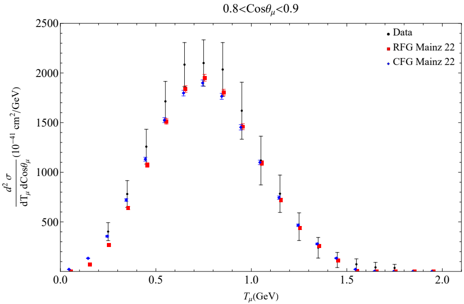

- **Fix axial form factor** and **vary nuclear models** in comparison to MiniBooNE data (Aguilar-Arevalo, *et al.*, Phys. Rev. D, 81:092005, (2010)).
- flux averaging ⇒ indistinguishable RFG, CFG cross-section data.

Neutrino Scattering: After flux averaging

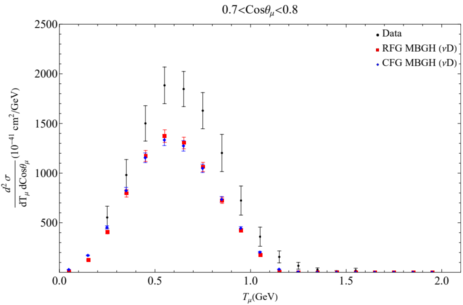

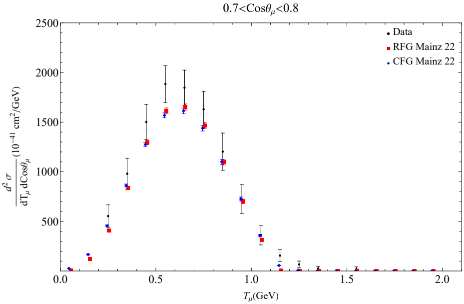

Neutrino Scattering: Axial form factor

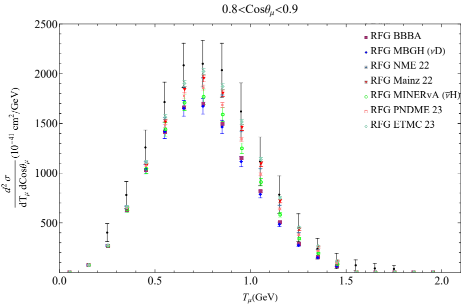

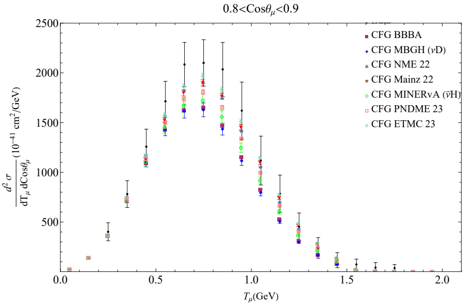

- **Vary axial form factor** and **fix nuclear model**.
- Continuous spread from F_A parameterizations for both nuclear models.

Neutrino Scattering: Axial form factor

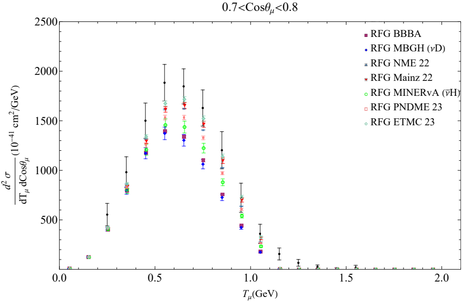

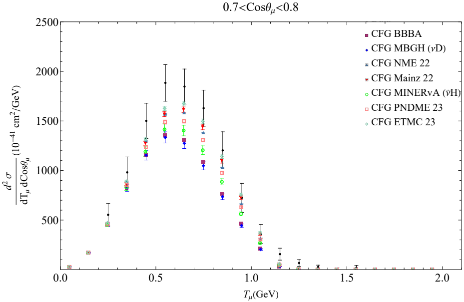

Summary

- Precision measurements $\Leftarrow$ better control of systematic uncertainties in lepton-nucleus interactions.

Summary

- Precision measurements $\Leftarrow$ better control of systematic uncertainties in lepton-nucleus interactions.
- QE lepton-nucleus scattering (ingredient):
  - scattering cross-section on a single nucleon: involving nucleon form factors
  - scattering cross-section off a nucleus (nuclear model): Correlated Fermi Gas model

Summary

- Precision measurements $\Leftarrow$ better control of systematic uncertainties in lepton-nucleus interactions.
- QE lepton-nucleus scattering (ingredient):
  - scattering cross-section on a single nucleon: involving nucleon form factors
  - scattering cross-section off a nucleus (nuclear model): Correlated Fermi Gas model
- Presented (arXiv: 2405.05342) fully analytic implementation of CFG model for CCQE lepton (e, ν)-nucleus scattering.

Summary

- Precision measurements ⇐ better control of systematic uncertainties in lepton-nucleus interactions.
- QE lepton-nucleus scattering (ingredient):
  - scattering cross-section on a single nucleon: involving nucleon form factors
  - scattering cross-section off a nucleus (nuclear model): Correlated Fermi Gas model
- Presented (arXiv: 2405.05342) fully analytic implementation of CFG model for CCQE lepton (e, ν)-nucleus scattering.
- Separately compare form factors and nuclear model effects: (e, ν)-carbon scattering data.

Summary

- Precision measurements $\Leftarrow$ better control of systematic uncertainties in lepton-nucleus interactions.
- QE lepton-nucleus scattering (ingredient):
  - scattering cross-section on a single nucleon: involving nucleon form factors
  - scattering cross-section off a nucleus (nuclear model): Correlated Fermi Gas model
- Presented (arXiv: 2405.05342) fully analytic implementation of CFG model for CCQE lepton (e, ν)-nucleus scattering.
- Separately compare form factors and nuclear model effects: (e, ν)-carbon scattering data.
- Electron scattering: distinguish two nuclear models; CFG model for small and large ω has a "tail". At the peak CFG prediction smaller than of RFG; difference between form factors small.

Summary

- Precision measurements $\Leftarrow$ better control of systematic uncertainties in lepton-nucleus interactions.
- QE lepton-nucleus scattering (ingredient):
  - scattering cross-section on a single nucleon: involving nucleon form factors
  - scattering cross-section off a nucleus (nuclear model): Correlated Fermi Gas model
- Presented (arXiv: 2405.05342) fully analytic implementation of CFG model for CCQE lepton (e, ν)-nucleus scattering.
- Separately compare form factors and nuclear model effects: (e, ν)-carbon scattering data.
- Electron scattering: distinguish two nuclear models; CFG model for small and large ω has a "tail". At the peak CFG prediction smaller than of RFG; difference between form factors small.
- Neutrino scattering: indistinguishable - two nuclear models using either MBGH or Mainz22; Mainz22 ($\approx m_A^{dipole,MiniBooNE}$) fits data much better than MBGH; almost continuous "spread" using F_A parameterizations for both RFG and CFG nuclear models.

Thank You!

Backup Slides

Backup Slides

Lepton and Hadron tensor

- The leptonic tensor is:

$$
\begin{aligned}
L^{\mu\nu}_{EM} &= 4(k^\mu k'^\nu + k^\nu k'^\mu - g^{\mu\nu} k.k') \\
L^{\mu\nu}_{Weak} &= 8(k^\mu k'^\nu + k^\nu k'^\mu - g^{\mu\nu} k.k' - i\epsilon^{\mu\nu\rho\sigma} k_\rho k'_\sigma)
\end{aligned}
$$

- The H_i's are expressed in terms of the form factors F_i as,

$$
\begin{aligned}
H_1 &= 8m_N^2 F_A^2 - 2q^2 \left[(F_1 + F_2)^2 + F_A^2 \right] \\
H_2 &= H_5 = 8m_N^2 \left(F_1^2 + F_A^2 \right) - 2q^2 F_2^2 \, , \\
H_3 &= -16 m_N^2 \, F_A (F_1 + F_2) \, , \\
H_4 &= -\frac{q^2}{2} \left(F_2^2 + 4F_P^2 \right) - 2m_N^2 F_2^2 - 4m_N^2 \left(F_1 F_2 + 2F_A F_P \right) .
\end{aligned}
$$

- The pseudo-scalar form factor related to F_A by Partial Conservation of Axial Current is:

$$
F_P(q^2) = \frac{2m_N^2}{m_\pi^2 - q^2} F_A(q^2)
$$

Correlated Fermi Gas

- We use the model by O. Hen, *et al.*, Phys. Rev. C, **91**, 025803:

$$n^{CFG}(\boldsymbol{p}) = \begin{cases} A_0 & |\boldsymbol{p}| \leq p_F \\ c_0 p_F / p^4 & p_F \leq |\boldsymbol{p}| \leq \lambda p_F \\ 0 & |\boldsymbol{p}| \geq \lambda p_F , \end{cases}$$

  where λ is the high momentum cut-off, p_F is Fermi momentum.
- The factor A_0 is determined by normalization:

$$1 = 2 \int \frac{d^3 p}{(2\pi)^3} n^{CFG}(\boldsymbol{p}),$$

$$\Longrightarrow A_0 = \frac{3\pi^2}{p_F^3} \left[1 - \left(1 - \frac{1}{\lambda} \right) \frac{c_0}{\pi^2} \right].$$

Limits of integration: RFG

Phys. Rev. D, **84**, 073006

- The definite integrals above have the limits $E_{\text{low}} \leq E_{\boldsymbol{p}} \leq E_{\text{high}}$
- only one transition possible $(\mathrm{I} \rightarrow \mathrm{IV})$
- first condition arises from the constraints on the scattering angle:

$$-1 \leq \cos\theta_{\boldsymbol{pq}} \leq 1 \quad \Rightarrow \quad -1 \leq \frac{\omega_{\text{eff}}^2 - |\boldsymbol{q}|^2 + 2\omega_{\text{eff}} E_{\boldsymbol{p}}}{2|\boldsymbol{q}|\sqrt{E_{\boldsymbol{p}}^2 - m_N^2}} \leq 1,$$

- The latter condition can be expressed as

$$\left(\frac{E_{\boldsymbol{p}}}{m_N} - \frac{cd + \sqrt{1 - c^2 + d^2}}{1 - c^2}\right)\left(\frac{E_{\boldsymbol{p}}}{m_N} - \frac{cd - \sqrt{1 - c^2 + d^2}}{1 - c^2}\right) \geq 0\,.$$

  Defining $\Delta \equiv m_N(cd + \sqrt{1 - c^2 + d^2})/(1 - c^2)$ this implies $\Delta \leq E_{\boldsymbol{p}}$.
- Therefore the limits for the RFG transition are:

$$\boxed{\mathrm{E}_{lo} = \max\Big(E_F - \omega_{eff}\,, \Delta\Big),\, E_{hi} = E_F\,.}$$

Semi-Inclusive Scattering

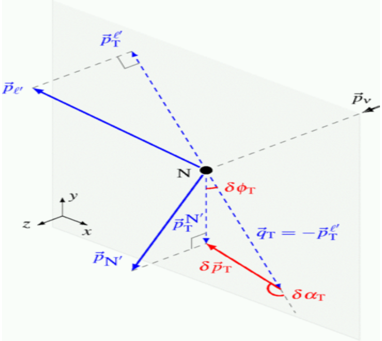

Figure: single-transverse kinematic imbalance (X. G. Lu, *et al.*, Phys. Rev. C, **94**, 015503 (2016))

$$\delta\vec{p}_T = \vec{p}_T^{\,l'} + \vec{p}_T^{\,N'},$$

$$\delta\alpha_T = \arccos\frac{-\vec{p}_T^{\,l'}\cdot\delta\vec{p}_T}{\vec{p}_T^{\,l'}\,\delta\vec{p}_T},$$

$$\delta\phi_T = \arccos\frac{-\vec{p}_T^{\,l'}\cdot\vec{p}_T^{\,N'}}{\vec{p}_T^{\,l'}\,\vec{p}_T^{\,N'}}$$

More plots

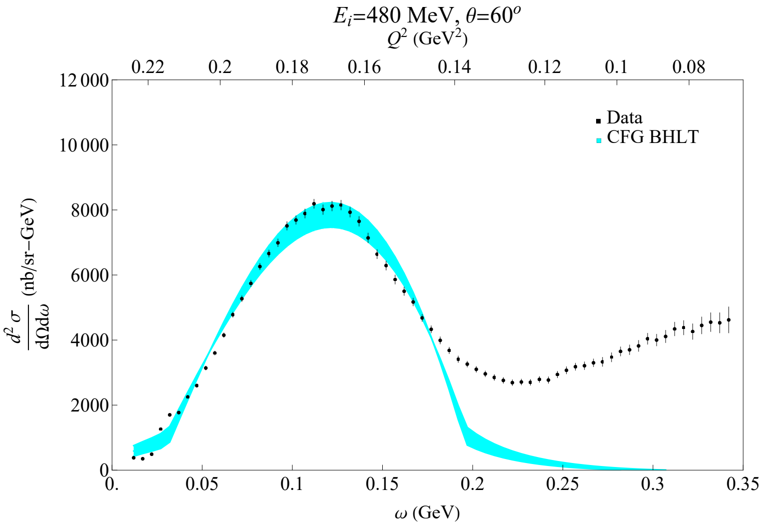
E_i=480 MeV, θ=60^o
Q^2 (GeV^2)
0.22
0.2
0.18
0.16
0.14
0.12
0.1
0.08
12 000
10 000
8000
6000
4000
2000
0
0.
0.05
0.1
0.15
0.2
0.25
0.3
0.35
$\frac{d^2\sigma}{d\Omega d\omega}$ (nb/sr–GeV)
ω (GeV)
Data
CFG BHLT

More plots

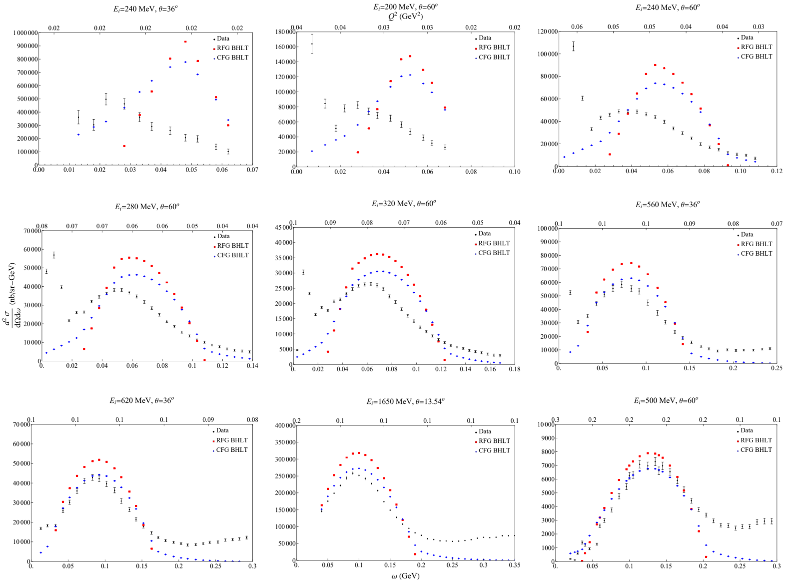
E_i=240 MeV, θ=36^o
E_i=200 MeV, θ=60^o
Q^2 (GeV^2)
E_i=240 MeV, θ=60^o
E_i=280 MeV, θ=60^o
E_i=320 MeV, θ=60^o
E_i=560 MeV, θ=36^o
E_i=620 MeV, θ=36^o
E_i=1650 MeV, θ=13.54^o
E_i=500 MeV, θ=60^o
Data
RFG BHLT
CFG BHLT
$\frac{d^2\sigma}{d\Omega d\omega}$ (nb/sr–GeV)
ω (GeV)

More plots: Responses ($\vec{q} = 300$ MeV)

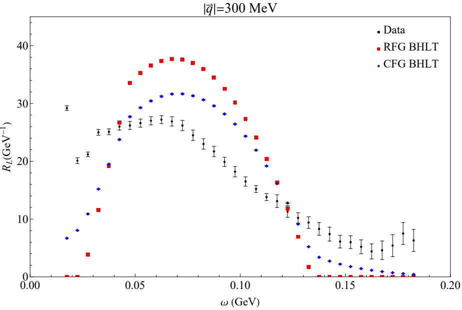

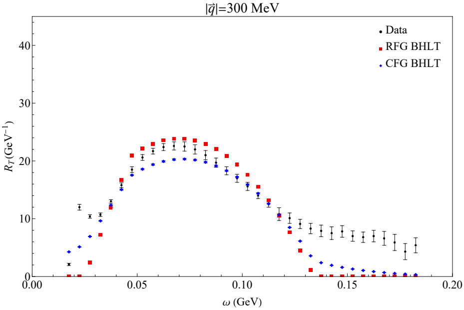

More plots: Responses ($\vec{q} = 400$ MeV)

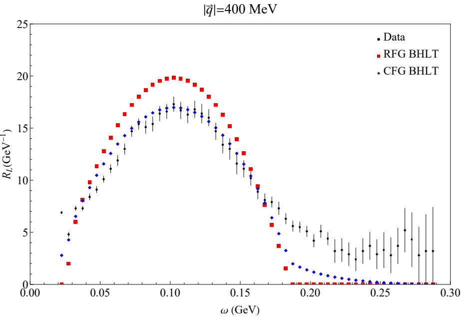

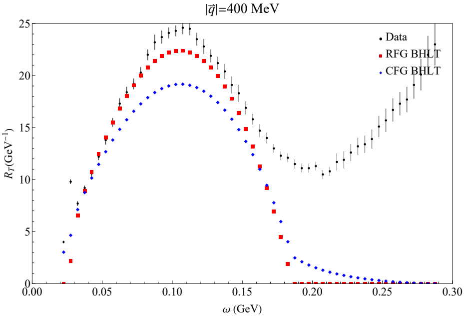

More plots: Responses ($\vec{q} = 550$ MeV)